

Comparative Study of Poloxamer Insertion into Lipid Monolayers[†]

Stacey A. Maskarinec and Ka Yee C. Lee*

Department of Chemistry, the Institute for Biophysical Dynamics, and the James Franck Institute, The University of Chicago, Chicago, Illinois 60637

Received July 1, 2002. In Final Form: November 7, 2002

Surface pressure versus area isotherms have been coupled with fluorescence microscopy to compare the insertion preferences of a series of triblock copolymers of the form poly(ethylene oxide)–poly(propylene oxide)–poly(ethylene oxide) (PEO–PPO–PEO) into dipalmitoylphosphatidylcholine (DPPC) and dipalmitoylphosphatidylglycerol (DPPG) monolayers at the air–water interface at 30 °C. Previous monolayer experiments with one of the polymers of the series, Poloxamer 188 (P188), which is known to effectively seal electrically damaged cell membranes, show that P188 is able to insert into model monolayer systems of DPPC and DPPG at surface pressures close to or lower than its maximal spreading pressure¹ of 22 mN/m at 30 °C. To test whether the size of the hydrophobic PPO subunit regulates the insertion capabilities of the polymer into the lipid films, we have investigated the effect of sister poloxamers P108, P238, and P338 that have identical PPO/PEO weight percentages as compared to P188 but differ in overall molecular weight. While the smallest polymer investigated, P108, is able to insert into the lipid films at a surface pressure equal to its maximal spreading pressure, the larger polymers, P238 and P338, can insert only at pressures much lower than their respective maximal spreading pressures. However, all polymers investigated are “squeezed out” or eliminated from both monolayers at surface pressures significantly higher than those for insertion, results which mirror those obtained for P188. Although the bulkiness of the larger polymers limits their ability to insert into the lipid monolayer at pressures close to their maximal spreading pressures, their larger hydrophobic subunits seem to help them maintain their positions in the monolayer once inserted.

Introduction

Disruption and permeabilization of the cell membrane are major constituents of significant radiation injury, thermal burns, frostbite, reperfusion injury, electrical shock, and many additional forms of trauma-mediated tissue damage.^{2,3} Therefore, understanding the biophysics of structurally compromised cell bilayers and subsequent sealing mechanisms is of vital importance to medical science.

Membrane sealing has been facilitated through the utilization of different types of synthetic surfactants. As a result of their amphiphilic nature, some surfactants have the capability to interact with a cell membrane, alleviating or reversing damage caused by disease or trauma. A particular triblock copolymer called Poloxamer 188 (P188, MW = 8400 g/mol) has been found to be successful as a surfactant sealing agent for permeabilized cell bilayers.^{4–8} P188 was first shown to be effective when it reduced the leakage of carboxyfluorescein dye from loaded cells after

electroporation.⁹ Further investigations showed that P188 was able to insert into bilayer pores formed in skeletal muscle tissue after heat shock¹⁰ and also helped to decrease the leakage of calcein dye from high-dose-irradiated isolated skeletal muscle cells.¹¹ More recently, P188 has been shown to reduce the number of painful episodes for patients suffering from sickle cell disease by interacting with the hydrophobic portions of red blood cell membranes, thereby blocking undesirable cell–cell and cell–protein adhesive contacts. This effect leads to a reduction in blood viscosity and thus enhanced microvascular blood flow.¹² In all the aforementioned studies, P188 incorporation into the cell membrane has been thought to be responsible for the observed effects.

To further elucidate the molecular properties responsible for P188's observed interaction with cell membranes, a recent study has modeled the outer leaflet of the cell membrane using a lipid monolayer at the air–water interface and measured P188's ability to insert into it.¹³ Results from this study point to the hydrophobic poly(propylene oxide) (PPO) subunit of P188 as the integral

[†] Part of the *Langmuir* special issue entitled The Biomolecular Interface.

(1) The maximal surface pressure is defined as the highest surface pressure attained when the concentration of poloxamer in the subphase approaches that given by the critical micelle concentration.

(2) Hannig, J.; Lee, R. C. *IEEE Trans. Plasma Sci.* **2000**, *28*, 97–101.

(3) Chang, D. C.; Reese, T. S. *Biophys. J.* **1990**, *58*, 1–12.

(4) Matsuura, Y.; Najib, A.; Lee, W. H., Jr. *Surg. Forum* **1966**, *17*, 86–88.

(5) Lee, R. C.; Myerov, A.; Maloney, C. P. *Ann. N.Y. Acad. Sci.* **1994**, *720*, 239–245.

(6) Merchant, F. A.; Holmes, W. H.; Capelli-Schellpfeffer, M.; Lee, R. C.; Toner, M. *J. Surg. Res.* **1998**, *74*, 131–140.

(7) Sharma, V.; Stebe, K.; Murphy, J. C.; Tung, L. *Biophys. J.* **1996**, *71*, 3229–3241.

(8) Terry, M. A.; Hannig, J.; Carrillo, C. S.; Beckett, M. A.; Weichselbaum, R. R.; Lee, R. C. *Ann. N.Y. Acad. Sci.* **1999**, *888*, 274–284.

(9) Lee, R. C.; River, L. P.; Pan, F. S.; Ji, L.; Wollmann, R. L. *Proc. Natl. Acad. Sci. U.S.A.* **1992**, *89*, 4524–4528.

(10) Padanilam, J. T.; Bischof, J. C.; Lee, R. C.; Cravalho, E. G.; Tompkins, R. G.; Yarmush, M. L.; Toner, M. In *Electrical Injury: A Multidisciplinary Approach to Therapy, Prevention, and Rehabilitation*; Annals of the New York Academy of Science, Vol. 720; New York Academy of Sciences: New York, 1994; pp 111–123.

(11) Hannig, J.; Zhang, D.; Canaday, D. J.; Beckett, M. A.; Astumian, R. D.; Weichselbaum, R. R.; Lee, R. C. *Radiat. Res.* **2000**, *154*, 171–177.

(12) Orringer, E. P.; Casella, J. F.; Ataga, K. I.; Koshy, M.; Adams-Graves, P.; Luchtman-Jones, L.; Wun, T.; Watanabe, M.; Shafer, F.; Kutlar, A.; Abboud, M.; Steinberg, M.; Adler, B.; Swerdlow, P.; Terregino, C.; Saccente, S.; Files, B.; Ballas, S.; Brown, R.; Wojtowicz-Praga, S.; Grindel, J. M. *JAMA, J. Am. Med. Assoc.* **2001**, *286*, 2099–2106.

(13) Maskarinec, S. A.; Lee, R. C.; Lee, K. Y. C. *Biophys. J.* **2002**, *82*, 1453–1459.

Table 1

poloxamer	MW	N_{PPO}	N_{PEO}^a
P108	4700	16	42
P188	8400	30	76
P238	11400	39	104
P338	14600	50	132

^a Number of PEO monomers in each of the two hydrophilic chains; MW = molecular weight in g/mol.

factor regulating the polymer's capabilities to interact and insert into the lipid films. If this premise is correct, then the actual size of the PPO subunit and/or the ratio of the PPO/poly(ethylene oxide) (PEO) subunits of the polymer should dictate its membrane sealing effectiveness.

To test whether the actual size of the PPO subunit of the polymer alone dictates the extent of polymer insertion into lipid films, a systematic study comprised of monolayer insertion and elimination experiments has been performed using sister poloxamers P108 (MW = 4700 g/mol), P238 (MW = 11 400 g/mol), and P338 (MW = 14 600 g/mol). This series of poloxamers has been chosen because it provides information on how the overall size of the poloxamer at a constant hydrophobic to hydrophilic chain proportion affects lipid–poloxamer interactions (see Table 1).

Using a model lipid system, we have carried out isotherm measurements and fluorescence microscopy imaging to examine and compare the interactions of the above-mentioned poloxamers with both zwitterionic (dipalmitoylphosphatidylcholine, DPPC) and anionic (dipalmitoylphosphatidylglycerol, DPPG) monolayers on a pure water subphase at 30 °C. These experiments examine the monolayer phase behavior and morphological changes associated with poloxamer incorporation, thus providing information on each poloxamer's insertion capabilities.

By measuring poloxamer insertion as a function of lipid packing density, we show that the two smallest poloxamers of the series, P108 and P188, are able to insert into both types of lipid films at surface pressures equal to or lower than their respective maximal spreading pressures of 18 and 22 mN/m. The larger poloxamers, P238 and P338, however, are unable to insert into monolayers at surface pressures corresponding to their maximal spreading pressure despite the fact that they contain 25 and 42% more hydrophobic units than P188, respectively. This observation indicates that even though the larger poloxamers have more hydrophobic subunits, the overall poloxamer size plays a crucial role in determining insertion aptitudes at high lipid packing densities. Once incorporated into the monolayers, however, P238 and P338 are able to retain their positions in a monolayer at the air–water interface at much higher surface pressures than the two smaller poloxamers, P108 and P188, before being squeezed out, leaving behind a pure lipid monolayer.

This collection of results suggests that the interaction capabilities of each poloxamer can be most accurately described by their insertion and elimination surface pressures, which do not necessarily correspond to their maximal spreading pressures on a pure water subphase. Morphologically, injection experiments performed at a constant area show an increase in lipid packing density as a result of poloxamer insertion.

Materials and Methods

Lipids and Subphase. DPPC and DPPG were purchased in chloroform-based aliquots from Avanti Polar Lipids, Inc. (Alabaster, AL). Monolayer spreading solutions were prepared by further dilution of the concentrated lipid aliquot in chloroform (high-performance liquid chromatography grade, Fisher Sci-

entific, Pittsburgh, PA) to obtain a concentration of 0.2 mg/mL. One mole percent of Texas Red, 1,2-dihexadecanoyl-*sn*-glycerol-3-phosphoethanolamine, triethylammonium salt (Molecular Probes Inc., Eugene, OR), was the fluorescent dye used for all experiments. For all trials, ultrapure water, made by using a combination of reverse osmosis (RiOs/Elix-10) and ultrapurification (Milli-Q, A-cogradient, Millipore, Bedford, MA), was used as the subphase.

Poloxamer Solutions. Solutions of 200 mg of each poloxamer (P108, P188, P238, P338) (BASF, Parsippany, NJ) per milliliter of ultrapure water were prepared by adding the poloxamer and water to a vial containing a magnetic stir bar and then left to mix on a stirplate for up to 2 h to ensure complete dissolution of the poloxamer. All poloxamer solutions were stored at 4 °C prior to use and made fresh weekly.

Langmuir Trough with Fluorescence Microscopy Attachment. All surface pressure–area isotherms were collected using a Teflon Langmuir trough equipped with a Wilhelmy plate (Reigler & Kirstein, Berlin, Germany). The home-built Teflon Langmuir trough (27.5 cm × 6.25 cm × 0.63 cm) equipped with two identical mobile Teflon barriers ($l = 6.25$ cm) enables compression or expansion of monolayers spread at the air–water interface, thereby increasing or reducing the surface pressure, respectively. The water subphase volume used is typically 95 mL, and the maximum working surface area is 145 cm². The subphase temperature is maintained within 0.5 °C of the desired temperature of 30 °C through the use of a home-built temperature control unit comprised of thermoelectric units (Omega Engineering Inc., Stamford, CT) joined to a heat sink held at 20 °C by a Neslab RTE-100 water circulator (Portsmouth, NH). A resistively heated indium tin oxide coated glass plate (Delta Technologies, Dallas, TX) is placed over the trough to minimize dust contamination, air currents, and evaporative losses and to prevent condensation of water on the microscope objective.

Our Langmuir trough is positioned on translation stages that permit scanning along the air–water interface in the x and y directions and focusing in the z direction. This assembly is fixed to a custom-built microscope stage for simultaneous fluorescence microscopy with a 50× long working distance objective lens (Nikon Y-FL, Fryer Co., Huntly, IL). Excitation between 530 and 590 nm and emission between 610 and 690 nm are gathered through the use of a filter cube (Nikon HYQ Texas Red, Fryer Co.). Images from the fluorescence microscope are collected at a video rate of 30 frames/s using a silicon intensified target (SIT) camera (Hamamatsu Corp., Bridgewater, NJ) and recorded on Super-VHS (S-VHS) formatted videotape with a recorder (JVC HR-S4500U, JVC Co. of America, Wayne, NJ). This assembly permits the monolayer morphology to be observed over a large lateral area while isotherm data are obtained concurrently.

The entire apparatus is set on a vibration isolation table (Newport, Irvine, CA) and is controlled using a custom software interface designed using LabView 4.1 (National Instruments, Dallas, TX).

Critical Micelle Concentration (cmc) Experiments. Using a method previously described,¹³ we first determined the critical micelle concentration of each poloxamer by examining its surface activity at the air–water interface. To quantify the cmc, separate experiments with an increasing amount of a 200 mg/mL poloxamer solution injected into the water subphase have to be performed. In a typical experiment, the system is left undisturbed for 30 min after poloxamer injection into the pure water subphase, and the rise in surface pressure over this time period is noted at the end of the period. The cmc for a particular poloxamer is determined when subsequent increases in poloxamer concentration do not result in a further rise in the surface pressure.

Lateral Compression Experiments. All experiments have been performed on pure water at 30 °C. Lipid monolayers are formed at the air–water interface through the deposition of a known volume of the monolayer spreading solution on the water surface using a microsyringe. Upon spreading, the lipid film is left undisturbed for 15 min to allow for solvent evaporation. At this point, barrier compression is initiated and the increase in surface pressure of the monolayer is monitored at 1 s time frames. This gives rise to a surface pressure (mN/m) versus area per lipid molecule (Å²/molecule) isotherm, which can be utilized to

deduce the phases and phase transitions associated with the monolayer as a function of lateral lipid packing density. Two different monolayer experiments have been performed: injection and pretreatment experiments. Injection experiments are designed to ascertain the specific lipid packing densities under which each poloxamer is able to incorporate itself into the lipid films, a reflection of the ease of surface adsorption and insertion as a function of surface pressure. Pretreatment experiments, on the other hand, test the inserted poloxamer's ability to sustain its position in the monolayer at higher lipid packing densities. In the context of cell membrane injury, such an increase in lipid packing density mimics the scenario where the integrity of the compromised cell membrane is re-established. Pretreatment experiments thus provide indications of the fate of the poloxamer upon cell healing after the injury.

Injection Experiments. The protocols for the injection experiments have previously been described elsewhere.¹³ We have performed two types of injection experiments, one at constant surface pressure and the other at constant surface area to determine the insertion capabilities of each poloxamer. In a constant pressure experiment, the lipid monolayer is first compressed to a surface pressure of 30 mN/m, resulting in a lipid packing density similar to that found in a normal cell bilayer. The surface pressure is held constant via a feedback loop built into the experimental apparatus. The poloxamer is then injected into the subphase and left undisturbed for 10 min to allow for insertion as signified by a change in area per molecule at a constant pressure. If no insertion is observed, the surface pressure is then lowered by 2 mN/m every 10 min. This reduction in lipid packing density creates a condition similar to that of a cell membrane whose integrity has been compromised. The surface pressure step-down continues until poloxamer incorporation is noted and the barriers are fully re-expanded.

For the constant area experiment, a lipid film is compressed to the onset insertion pressure found in the constant pressure injection experiments. The barriers are rendered immobile, and the poloxamer is added to the subphase to allow for an increase in surface pressure at a constant area. The film is monitored over a 2 h period, and changes in surface pressure are recorded with respect to time.

During the course of both constant pressure and constant area injection experiments, fluorescence microscopy (FM) images of the surface morphology are recorded on S-VHS videotape as mentioned previously.

Pretreatment Experiments. Pretreatment experiments were performed as described in ref 13 to detect if the poloxamer could remain incorporated in the lipid film at high lipid packing densities. In a typical experiment, a monolayer of the desired lipid is first deposited at a low surface density, such that the surface pressure of the film remains zero after spreading. Upon solvent evaporation, the poloxamer under investigation is injected into the subphase (at $\pi = 0$ mN/m) and the system is left undisturbed for 5 min. The film is then compressed to collapse, and the observed phase behavior of the system is compared to that when no poloxamer is present.

Image Grabbing and Handling. Static images were transferred to the computer from the S-VHS tape as 640 pixel \times 480 pixel bitmap images (BMP) using an 8 MB All-in-Wonder Pro Card (ATI Technologies, Thornhill, ON, Canada). These images were subsequently resized and enhanced in brightness and contrast for visual clarity.

Results and Discussion

Critical Micelle Concentration Results. To perform all experiments for polymer insertion into lipid monolayers below the cmc of each poloxamer, experiments to identify the cmc were first performed. The cmc for P188 has previously been found to be 1.25×10^{-4} M.¹³ Our data indicate that the cmc's for P108, P238, and P338 are approximately 2.90×10^{-4} , 1.02×10^{-4} , and 4.70×10^{-5} M, respectively. All subsequent poloxamer insertion experiments have been performed at poloxamer concentrations below the cmc of the respective poloxamer to avoid micellization. By addition of only 200 μ L of each of the 200

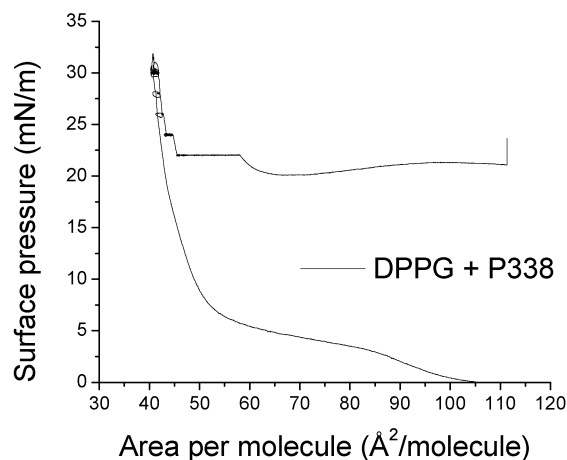


Figure 1. Injection of P338 into the water subphase of a DPPG monolayer at 30 °C. Monolayer films were compressed to 30 mN/m before P338 was injected into the subphase. No change in area per molecule was observed at 30 mN/m, so the pressure was lowered by 2 mN/m, and the monolayer was observed for 10 min to allow for insertion. As no insertion was observed, the surface pressure lowering procedure was continued until a small level of insertion was noted at 24 mN/m. A significant amount of insertion was observed when the surface pressure was reduced to 22 mN/m. When the pressure was further lowered to 20 mN/m, the barriers expanded to their original pre-compression position, which was designated as the end point of the experiment. At each surface pressure, the monolayer was observed for 10 min to allow for insertion.

mg/mL poloxamer solutions, it can be assumed that all of the poloxamer goes to the surface and that the subphase volume change on injection is negligible.

Lateral Compression Results. Isotherm and surface morphology measurements previously performed on pure DPPC and DPPG monolayers¹³ form the basis for observing phase and morphological changes as a result of poloxamer–lipid interaction. Any deviations from the characteristics observed in DPPC and DPPG isotherms and the morphology obtained in the absence of poloxamer are attributed to the presence of poloxamer at the air–water interface.

Injection Results. For constant surface pressure experiments, DPPC and DPPG monolayers were compressed until they reached 30 mN/m. The films were then held at this surface pressure while the desired poloxamer was administered to the subphase. No immediate change in the area per molecule or morphology was observed at 30 mN/m for a period of 10 min for any combination of lipid and poloxamer. Consequently, the surface pressure was lowered to 28 mN/m. Again, no observable change was detected for any poloxamer–lipid system at this reduced surface pressure. A 2 mN/m surface pressure step-down procedure was then adopted until a low level of P338 insertion was observed for the DPPG monolayer at 24 mN/m (see Figure 1). Since this change in the effective area per lipid molecule was only marginal for DPPG after 10 min, the surface pressure was lowered again to 22 mN/m, where there was a change in surface area of 14 Å²/molecule over the period of 10 min. The surface pressure of the system was further reduced to 20 mN/m where significant P338 insertion into the DPPG monolayer was detected (see expansion in Figure 1 and data in Table 2). At this pressure, which we denote as the insertion pressure, the barriers were fully re-expanded by 52 Å²/molecule to the precompression position within 30 min. Similar insertion behavior was noted for P338 incorporation into the DPPC monolayer, demonstrating an insertion pressure of 18 mN/m and a surface area change of 28

Table 2.^a

poloxamer	MSP	lipid	constant Π		constant A ΔA	pretreatment squeeze-out Π
			insertion Π	ΔA		
P108	18–20	DPPC	18	56	4	30
		DPPG	18	68	6	29
P188	20–22	DPPC	20	66	4	25
		DPPG	20	74	6	28
P238	23–25	DPPC	18	44	4	34
		DPPG	20	51	6	35
P338	26–28	DPPC	18	28	8	35
		DPPG	20	52	6	36

^a MSP = maximum spreading pressure; π is measured in mN/m; A = area per molecule ($\text{\AA}^2/\text{molecule}$).

$\text{\AA}^2/\text{molecule}$ (isotherm not shown, see Table 2 for data). P338 insertion for both films occurred at surface pressures 6–10 mN/m lower than the maximal spreading pressure for P338 on a clean interface (see Table 2).

The morphological images of DPPG monolayers on a water subphase at 30 °C before and after the administration of P338 are shown in panels A and B of Figure 2, respectively. Before P338 injection, the condensed flower-shaped domains of DPPG occupy the dominant fraction of the liquid-expanded/condensed (LE/C) phase coexistence at 30 mN/m (Figure 2A). Upon the insertion of P338 at 20 mN/m, the condensed domains appear stretched and bent, forming a complex pattern of associated domains similar to those found for all investigated poloxamers in DPPG films (Figure 2B). In addition, there is a drastic increase in the percentage of LE or disordered phase, indicating the disordering of lipid packing by the insertion of the poloxamer. For P338-treated DPPC monolayers, the insertion of P338 causes the condensed domains to disintegrate, creating a homogeneous LE phase. These morphological observations match those obtained for monolayers treated with P108, P188, and P238 (data not shown).

Constant pressure experiments with P238 for both DPPC and DPPG monolayers display comparable results to those collected for the P338 trials. Insertion pressures of 18 and 20 mN/m are noted for DPPC and DPPG monolayers, respectively, a 3–7 mN/m difference from the maximal spreading pressure of P238 on pure water (see Table 2).

Analogous to constant pressure results obtained for the other three poloxamers investigated, the smallest poloxamer, P108, is unable to insert into DPPC and DPPG monolayers at a surface pressure of 30 mN/m. The surface pressure has to be reduced to 18 mN/m for both DPPC and DPPG films before considerable P108 insertion can be observed (see Table 2). Unlike P238 and P338 whose insertion pressures are substantially lower than their maximal spreading pressures, this insertion pressure of P108 corresponds to its maximal spreading pressure obtained on a pure water subphase.

For constant area experiments, the lipid monolayers were first compressed to a surface pressure that has demonstrated moderate to significant insertion for each respective poloxamer in the constant pressure experiments. The barriers were then left at a fixed position while the desired poloxamer was administered into the subphase. Increases in surface pressures due to poloxamer insertion were monitored over a 2 h period (see Table 2). Of the four poloxamers, P338 shows the largest increase in surface pressure upon poloxamer insertion. Figure 3 displays the constant area results for the P338-treated monolayers. For both DPPC and DPPG monolayers, there are drastic increases in the surface pressure upon the

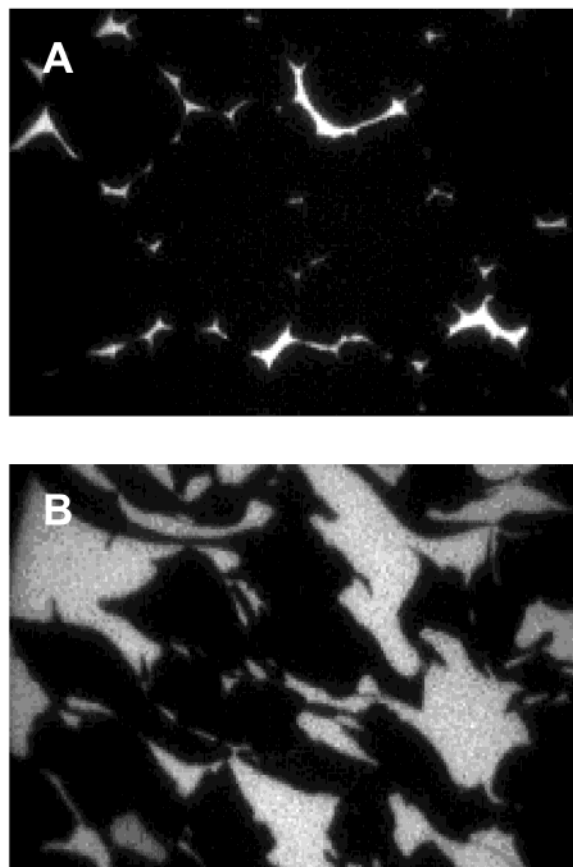


Figure 2. Fluorescence images during the P338 injection experiment into a DPPG monolayer at 30 °C on a water subphase. (A) The DPPG monolayer before P338 injection at 30 mN/m, which shows that the area covered by the condensed phase (bright) is substantially more than that of the fluid phase (dark). (B) The DPPG monolayer after P338 insertion at a surface pressure of 20 mN/m. There is a significant decrease in the amount of condensed phase and a corresponding increase in the amount of fluid phase. P338 incorporation into the monolayer causes the condensed phase domains to become elongated. The width of the image is 200 μm .

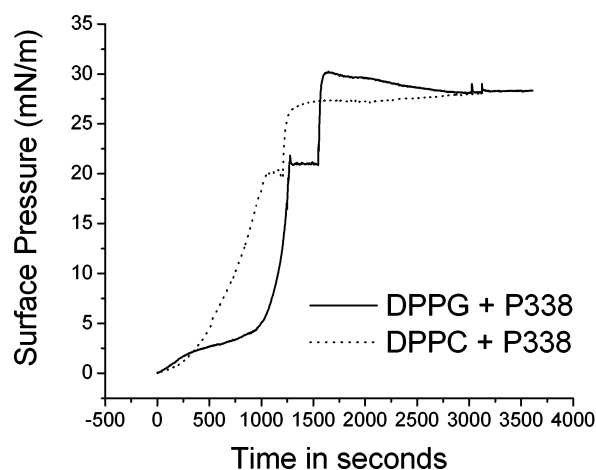


Figure 3. Constant area measurements of DPPC and DPPG monolayers after P338 injection at 20 mN/m for DPPC and 22 mN/m for DPPG at 30 °C on a water subphase. The surface pressure increases by 8 mN/m for DPPC and 6 mN/m for DPPG.

addition of P338 into the subphase (see sharp jumps in Figure 3). A final surface pressure of 28 mN/m is reached for both DPPC and DPPG monolayers.

Corresponding morphological images for the DPPC monolayer on pure water at 30 °C before and after P108

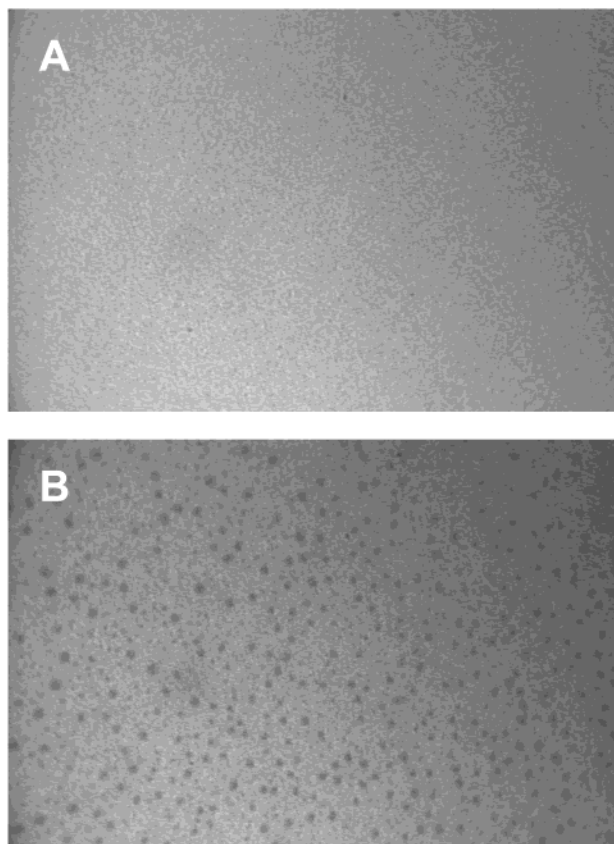


Figure 4. Fluorescence images during the P108 injection experiment at constant area into a DPPC monolayer at 30 °C on a water subphase. (A) The DPPC monolayer before P108 injection at 18 mN/m, displaying a homogeneous LE phase. (B) The DPPC monolayer after P108 insertion; the surface pressure increased from 18 to 22 mN/m. The incorporation of P108 into the lipid film and the subsequent increase in the surface pressure have caused the onset of the LE/C phase transitions as demonstrated by the formation of darkened condensed domains suspended in a bright fluid phase. The width of the image is 220 μm .

injection are shown in panels A and B of Figure 4, respectively. Before P108 injection, the DPPC monolayer at 18 mN/m is entirely in the LE phase (Figure 4A). The addition of P108 into the subphase, its insertion into the film, and the subsequent increase in surface pressure facilitate the onset of the LE \rightarrow C phase transition of the DPPC monolayer as demonstrated by the nucleation of condensed phase domains in Figure 4B. This result suggests that the incorporation of P108 into the film at its insertion pressure leads to the formation of a more densely packed film.

Pretreatment Results. In pretreatment experiments, the lipid was spread at a high area per molecule ($\tau \approx 0$ mN/m), and the desired poloxamer was added to the system to allow for maximum insertion. For both DPPC and DPPG monolayers, the addition of poloxamer to the subphase results in the partitioning of the poloxamer to the air–water interface, which gives rise to an instantaneous increase in surface pressures from 0 mN/m to the maximal spreading pressure of each poloxamer (see Table 2). The heterogeneous lipid–poloxamer system was then compressed until collapse. Figure 5 shows results obtained for the P338-pretreated DPPC monolayer. Beyond a surface pressure of 35 mN/m, the isotherm of the P338-pretreated monolayer reverts to that of a pure DPPC monolayer, suggesting that P338 has been eliminated from the film (Figure 5). For all poloxamers used and for both

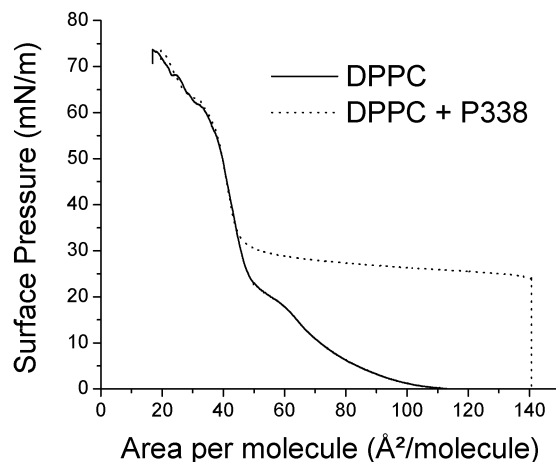


Figure 5. Lateral compression isotherms of DPPC and P338-pretreated DPPC on a water subphase at 30 °C. At surface pressures of 35 mN/m and greater, the isotherm of the P338-treated systems overlaps that of the pure lipid, indicating that P338 is squeezed out of the film at higher surface pressures equal to 35 mN/m or greater. The shoulder observed at high surface pressures is likely due to leakage of the trough.

lipid systems, the poloxamers are not completely squeezed out of the monolayer until surface pressures much higher than the poloxamers' respective insertion surface pressures are reached (see Table 2). In particular, the larger polymers P238 and P338 can stay within the lipid monolayer until a surface pressure of at least 34 mN/m is reached. Our data indicate that although it is more difficult for the larger polymers P238 and P338 to insert into monolayers at high surface pressures, once incorporated into the lipid monolayer, they can retain their positions within the monolayer until a much higher lipid packing density is reached. We do not include any FM image for the pretreatment experiments because the addition of the poloxamer at such a high molecular area does not result in any discernible surface morphology.

Conclusion

Our previous work on P188–lipid interaction points to the possible role of the hydrophobic poloxamer subunit in determining the ease and extent of the poloxamer's ability to insert into and retain its position in a lipid monolayer. To investigate the molecular properties responsible for the observed membrane sealing abilities of triblock copolymer surfactants and how the effective size of the PPO subunit affects the insertion characteristics of the polymer, we have performed a comparative study on a series of sister poloxamers of P188 with model monolayers of DPPC and DPPG using a Langmuir trough. All of the poloxamers examined, P108, P188, P238, and P338, consist of 80% hydrophilic PEO and 20% hydrophobic PPO but differ only in the overall molecular size (molecular weight ranging from 4700 to 14 600 g/mol). By examining the insertion and interaction preferences of this series of poloxamers, we are able to deduce that the actual size of the hydrophobic PPO unit alone is not always the limiting factor regulating poloxamer insertion into lipid films.

While all poloxamers examined are able to insert into both DPPC and DPPG monolayers, they exhibit different insertion behavior. Despite the higher maximal surface pressures of the larger poloxamers and the large number of hydrophobic PPO monomer units present in P238 and P338, their abilities to insert into lipid monolayers in constant pressure injection experiments are very similar to those of the smaller poloxamers, P108 and P188. For

all poloxamers examined, the surface pressure of the lipid monolayer, be it DPPC or DPPG, has to be lowered to the 18–20 mN/m range before substantial insertion can be observed. The bulkiness of the hydrophobic portion of the larger polymers likely hinders their insertion capabilities. A small but significant amount of insertion does commence at surface pressures slightly higher than the insertion pressures tabulated for all the poloxamers examined (see Table 2). While this small initial insertion is important in the context of sealing compromised cell membranes, the lower surface pressures are reported as they are the endpoint values as defined by our experimental protocol. The fact that all these polymers insert into the lipid monolayers only when the surface pressure of the film is much lower than the normal bilayer equivalent pressure (30–35 mN/m) indicates that they will adsorb only onto damaged portions of the cell membrane. Because the polymers interact only with parts of the bilayer whose packing densities have been compromised, thereby localizing their effects to needed areas, one can be rid of any worry that the poloxamers might nonspecifically insert into normal, healthy membranes. Moreover, similar injection results for DPPC and DPPG monolayers suggest that poloxamer insertion is not influenced by headgroup electrostatics.

Results from the constant area injection experiments show that all poloxamers except for P338 lead to a slightly higher increase in surface pressure for DPPG than DPPC monolayers. P338 also differs from the other poloxamers in that it is able to induce by far the largest increase in surface pressure upon insertion into DPPC monolayers (8 mN/m compared to 4 mN/m by other poloxamers). While it is not clear what causes P338 to behave somewhat differently from its smaller sister poloxamers, it is not surprising that the poloxamer with the highest maximal spreading pressure can impart a greater surface pressure increase on the lipid film upon its insertion. It is also interesting to note that for the two larger poloxamers, the endpoint surface pressures attained in these constant area injection experiments are actually higher than the maximal spreading pressures of the poloxamers. These results clearly indicate that poloxamers can effectively insert into the injured region where the local lipid packing density is reduced. Judging from the resulting increase in surface pressure, the insertion of poloxamers helps increase the lipid packing density of the damaged cell membrane.

Although the bulkiness of the hydrophobic portion of the large poloxamers hinders their initial ability to insert into the lipid monolayer (as demonstrated in the constant pressure injection experiments), they, when compared to the smaller polymers, can more effectively retain their positions in the lipid film until much higher surface pressures are attained. Nonetheless, at high enough surface pressures, results from pretreatment experiments clearly demonstrate that all poloxamers are “squeezed out” of the film. The elimination of the once-inserted poloxamers from the interface results in a pure DPPC or DPPG lipid monolayer, as shown by the complete overlap of isotherms with and without P338 at surface pressures beyond 35 mN/m (Figure 5). The inability of the poloxamers to stay within the monolayer at high surface pressures is reassuring as it points to the possible fate of the poloxamers should the damaged cell regain its integrity. In fact, this provides a mechanism for the graceful exit of the poloxamer that once helped seal the leaky damaged membrane when its presence is no longer needed. This eliminates the possibility that the inserted polymer may interfere with the self-healing process of the cell.

It is true that a monolayer can at best represent one leaflet of the cell membrane, but results obtained in this type of model system can provide some insight concerning the interaction between poloxamers and lipid bilayers. The loss of structural integrity of the cell membrane can likely manifest itself as a reduction in lipid packing density or by the formation of pores and subsequent intracellular material loss. In the work presented here, we try to mimic these conditions by using lipid monolayers. The former situation is modeled using the insertion assay where lipid molecules are first compressed to a lipid packing density equivalent to that found in a normal bilayer, followed by a systematic lowering of the surface pressure thereby reducing the lipid packing density, imitating the loss of membrane integrity. The latter condition is simulated by the pretreatment experiment that evaluates the behavior of the poloxamer when presented to a film in the gas–liquid coexistence at zero surface pressure. In this case, the gaseous phase effectively resembles pores in the film. We therefore trust that these monolayer results reflect the ease of polymer insertion and the ability of inserted poloxamers to remain in the lipid film as a function of molecular weight and can be translated to behavior in lipid bilayers. With the monolayer representing only a half-space of the lipid bilayer, there are certain aspects of poloxamer–bilayer interactions such as the mode of polymer insertion or the conformation of the inserted poloxamer that cannot be adequately addressed using a monolayer system. Examinations of these aspects of interaction are currently under way in our laboratory through the utilization of supported bilayers and unilamellar vesicles as model systems.

In conclusion, we attempt in this study to address the question of how the molecular properties of the poloxamer can regulate its membrane-sealing capability by examining the possibility of tuning the insertion profile by means of altering the molecular weight of the poloxamer while maintaining the hydrophobic-to-hydrophilic ratio. Our experimental data lead us to two seemingly different conclusions. On one hand, increasing the absolute size of the hydrophobic subunit renders the polymer bulky and deters its ability to insert into the lipid monolayer, suggesting that increasing the molecular weight of poloxamers does not enhance the poloxamer’s performance. On the other hand, the larger poloxamers, upon inserting into the lipid monolayer, are able to remain associated within the film until a much higher lipid packing density is reached. What remains to be determined is how to improve upon the polymer’s insertion characteristics (such that the lipid packing density of the damaged membrane does not have to be lowered significantly before insertion of the poloxamer occurs) without comprising the ability of the poloxamer to sustain its position in the film until normal lipid packing densities are achieved. As a first step, we are trying to gain a better understanding of the triblock copolymer conformation by carrying out molecular dynamic simulations under both implicit and explicit solvent conditions. Should we be successful in determining the molecular attributes that help regulate the poloxamer’s insertion capability, more effective poloxamers can be specifically designed to seal membranes depending on the cell membrane composition, degree of damage, and injury type.

Acknowledgment. The authors thank Dr. Raphael C. Lee for introducing us to the subject of poloxamers as membrane sealants. K.Y.C.L. is grateful for the support from the Packard Foundation (Grant No. 99-1465). S.A.M. was supported by the Camille and Henry Dreyfus New

Faculty Award (Grant No. NF-98-048) which helps promote undergraduate research in the chemical sciences. The experimental apparatus was made possible by a NSF CRIF/Junior Faculty Grant (Grant No. CHE-9816513). S.A.M. thanks Ajaykumar Gopal and Canay Ege for

valuable input and experimental help. The authors are grateful to Ajaykumar Gopal and Josh Kurutz for help with the manuscript.

LA026175Z